submitted to the 4th European Conference on Turbomachinery, Florence, Italy, 20−23 March 2001

EFFECTS OF GEOMETRY ON THE FLOW AND HEAT TRANSFER IN A ROTATING CAVITY WITH A STATIONARY OUTER CASING AND PERIPHERAL FLOW

Abdul Aziz Jaafar*, Michael Wilson and J. Michael Owen
Department of Mechanical Engineering
Faculty of Engineering and Design
University of Bath
Bath BA2 7AY, UK

*now at Aerospace Engineering Department, Faculty of Engineering,
University of Putra Malaysia
43400 UPM − Serdang, Selangor, Malaysia

ABSTRACT

Simplified rotating cavities can be used to model the flow in the internal air−cooling systems used in gas turbine engines. In this paper, experimental and computational results are presented for the flow and heat transfer in a system comprising two corotating discs, a rotating cylindrical hub and a stationary outer casing. Three cross−section shapes have been considered for the casing: flat, angled and stepped. One of the rotating discs is heated, a superposed flow of cooling air is introduced through nozzles at the periphery of the system, and air leaves through clearances at the casing. The purpose of the present work is to identify the effects of the different casing geometries on the flow and heat transfer occurring in the cavity.

Axisymmetric computations for each system, assuming incompressible, steady flow, have been carried out using a commercial computational fluid dynamics code, employing a high−Reynolds−number k−ε turbulence model and wall−functions. Reasonably good agreement is obtained between computed and measured values of Nusselt number, although there is poor agreement betwen computed and measured velocity distributions in some cases. Possible reasons for these discrepancies are discussed.

The results indicate that the geometry of the outer casing affects the secondary flows inside the cavity, set up by the shear between the rotating fluid and the casing. Tangential velocity distributions are found to be less sensitive to the details of the geometry. The effects on Nusselt numbers for the heated disc are also small, except where inlet flow angled towards the heated disc causes separation of the disc boundary layer. The effects of rotational speed and flow−rate on heat transfer for the angled casing configuration are also described.

INTRODUCTION

In some gas−turbine cooling systems, a peripheral flow of cooling air is introduced either through nozzles in a stationary outer casing, as illustrated in Fig. 1a,b, or through holes in a rotating disc (Fig. 1c); the air leaves the system through clearances in the outer casing, as illustrated. Referring to Fig. 1a, tangential shear at the stationary outer casing reduces the angular momentum of the rotating fluid, giving rise to radially−outward pumping on the discs. The flows from the disc boundary layers meet along the outer casing; these then form a free shear flow directed inward between the discs.

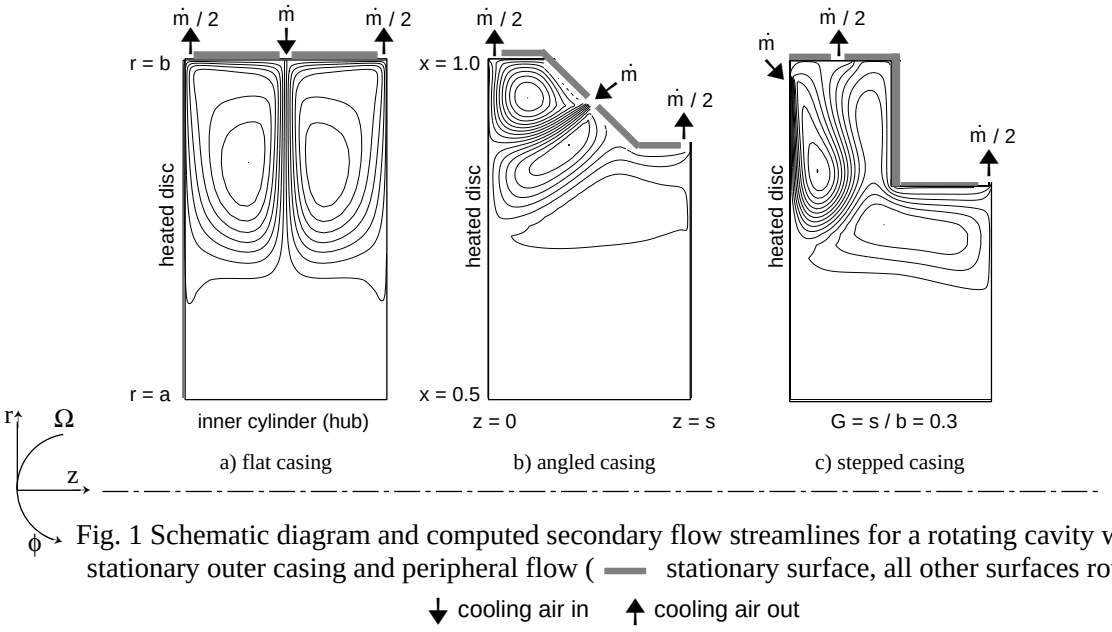

Fig. 1 Schematic diagram and computed secondary flow streamlines for a rotating cavity with a stationary outer casing and peripheral flow (▬ stationary surface, all other surfaces rotate)

Gan et al [1] carried out experiments and computations for the rotating cavity shown in Fig. 1a. For a sealed system (i.e. with no superposed cooling flow) it was found that the inward penetration of the recirculating secondary flows reduced with increasing rotational Reynolds number, $Re_\phi = \Omega b^2/\nu$. Increasing the magnitude of the turbulent flow parameter, λ_T , increased the inward penetration ($\lambda_T = C_w Re_\phi^{-0.8}$, where $C_w = m/\mu b$ is the nondimensional superposed flow−rate; by convention, $\lambda_T < 0$ when the cooling air is directed inward). Radial distributions of tangential velocity, measured outside the boundary layers on the discs, were found to follow combined free and forced (or Rankine) vortex behaviour. Steady axisymmetric computations, carried out using the Launder−Sharma k−ε turbulence model, gave poor predictions of this behaviour for the sealed case. (Owen [2] reviewed this and other research into the flow structure in a sealed rotating cavity with a stationary flat casing, for which instabilities in the free shear layers can give rise to unsteady three−dimensional flow. The effect of a superposed peripheral flow on such instabilities has not yet been studied.)

Gan et al found that agreement between computed and measured tangential velocities improved with increasing $|\lambda_T|$, as the fluid entered with zero swirl and reduced the rotation−rate of the fluid inside the cavity. However, the strength and inward penetration of the free−shear flow was then over−predicted, in comparison with measured axial distributions of radial velocity. Both computations and measurements indicated little axial variation in tangential velocity outside the boundary layers on the discs.

Mirzaee et al [3] addressed some of the uncertainties identified in the work of Gan et al, and also conducted measurements and computations of heat transfer for superposed flow cases. Surface roughness (due to the material used to insulate the cylindrical hub and outer casing surfaces) was shown to have reduced the level of tangential velocity measured in the system, but did not affect the underlying Rankine vortex structure. An empirical Richardson−number correction to the Launder−Sharma turbulence model gave some improvements to tangential velocity predictions for $\lambda_T = 0$, but did not correct the over−prediction of the radially−inward flow for superposed flow cases. Both computations and measurements showed that Nusselt numbers for the one heated disc (see Fig. 1a) increased with both Re_ϕ and $|\lambda_T|$. Measured local Nusselt number distributions were reasonably well predicted (when the effects of radiation from the heated disc and conduction through the adjacent unheated disc were accounted for in the computations), although the measured heat

transfer rates in the outer part of the system were underestimated.

Mirzaee et al [4] described a similar heat transfer study for the stepped−casing configuration (Fig. 1c), and identified different secondary flow recirculations for cases with low or high values of $|\lambda_T|$ respectively. It was again found, both computationally and experimentally, that Nusselt numbers for the heated disc increased with both Re_ϕ and $|\lambda_T|$. Jaafar et al [5] extended the heat transfer study of Mirzaee et al by making comparisons between computed velocities and laser−Doppler anemometry (LDA) velocity measurements. Computed tangential velocities, outside the disc boundary layers, were generally found to be higher than those observed experimentally. By contrast, the agreement between computed and measured Nusselt numbers was reasonably good, suggesting that the disc boundary layers may be predicted somewhat more accurately than the bulk flows in the cavity interior.

Extensive experimental studies of flow and heat transfer for the angled casing configuration, shown in Fig.1b, have also been carried out, and axisymmetric computations for all three of the systems shown in Fig. 1 were made by Jaafar [6] using a general−purpose code (PHOENICS) and a high−Reynolds−number k−ε turbulence model with wall−functions. "Flat casing" (Fig. 1a) computations confirmed the flow and heat transfer results obtained by Mirzaee et al [3] as described above, and results for the "stepped casing" were also very similar to those described by Jaafar et al [5], which were obtained using the Launder−Sharma turbulence model and a research code.

Jaafar et al [7] discussed the fluid dynamics for the "angled casing" configuration, and concluded, from the results of computations in which the main flow parameters were varied, that, as for the other systems described above, the flow structure was determined mainly by the magnitude of $|\lambda_T|$. For high values (as in the case illustrated in Fig. 1b), the secondary flows were characterised as "inertially−dominated", and the powerful inlet flow controls the secondary flow recirculations in the outer part of the cavity. At low values of $|\lambda_T|$, the inlet flow is entrained into the boundary layer on the angled surface of the casing, and the flow was said to be in a "viscous−regime".

In this paper, new computational results are presented for the flow and heat transfer for each of the flat, angled and stepped casing configurations described above. Brief descriptions only are given of the experimental apparatus and computational models, as these have been described in more detail elsewhere. Comparisons between computed and measured results for the different geometries are presented and discussed, in order to investigate the influence of the casing geometry (and peripheral flow arrangements) on the flow structure and heat transfer. The effects of rotational speed and cooling−air flow−rate on heat transfer for the angled casing configuration are also considered, complementing the previously−published work by Jaafar et al [7] for the fluid dynamics of this system.

EXPERIMENTAL APPARATUS

The rig described by Gan et al [1] was used for both the flat casing and angled casing studies described here, the only major difference being the fitting of the alternative casings. The dimensions of the rotating cavity (see Fig. 1) were b = 382 mm and s = 113 mm (giving a gap ratio G = s/b = 0.3), and the hub radius ratio was given by a/b = 0.5. The inclined face of the angled casing was at 45°, with its inner cylindrical surface at a radius of 331 mm. Cooling air was supplied through 38 nozzles, each of 11.3 mm diameter and with axes normal to the face of the casing in the r−z plane. The nozzles could be angled in the tangential direction to impart swirl to the flow at inlet, characterised by the inlet swirl ratio $c = V_{\phi,in}/\Omega b$. More details are given by Gan et al [1] and Mirzaee et al [3] for the flat casing, and by and Jaafar et al [7] for the angled casing. The maximum rotational speed was around 1500 rev/min.

Mirzaee et al [4] described the modifications made to the rig for the stepped casing studies. A carbon−fibre nozzle ring was attached to the periphery of the heated rotating disc, having 74 holes each of 8.6 mm diameter and inclined at 24° to the radial direction in the r−z plane. The flow was assumed to enter the cavity through the rotating holes with inlet swirl c = 1. The inner and outer cylindrical surfaces of the stepped casing were at 335 mm and b = 411 mm respectively, and its radial face was mid−way between the discs; the gap ratio G = 0.3 and radius ratio a/b = 0.5 used in earlier studies were maintained. Fig. 1c shows the modified outlet locations. For each of the three configurations, the flow−rates at the two outlets could be controlled; for all of the results described here, the flow−rates at the two outlets were equal.

Heat transfer measurements were made for the left−hand disc (see Fig. 1). The disc was made from steel, was instrumented with thermocouples and fluxmeters and could be heated to around 100°C by stationary radiant heaters, while the hub and outer casing surfaces were insulated. (The surface roughness of the insulating material, Rohacell, was found to have had a significant effect on some velocity measurements, as explained below.) The right−hand unheated disc was made from polycarbonate, providing optical access for laser−Doppler anemometry (LDA). All of the velocity measurements were made under isothermal conditions; more details are given by Gan et al [1] and Jaafar et al [5]. More details of heat transfer measurements are given by Mirzaee et al [3,4].

COMPUTATIONAL MODEL

The PHOENICS models used for the different configurations considered here are all similar to that described by Jaafar et al [7] specifically for angled casing computations. Block obstructions were used to represent the angled or stepped casing cross−sections on an axisymmetric, non−uniform cylindrical−polar grid. For the angled surface, a step−wise approximation was employed which was believed to be sufficiently realistic given the resolution afforded by the high Reynolds−number k−ε wall−function turbulence model. Hybrid differencing was used for convective terms. Near−wall cells were located so that y^+ values of around 30 were obtained over most of the disc and outer casing surfaces. Following grid sensitivity studies, a 93x93 (axial x radial) mesh was used for the stepped and angled casing geometries. For the flat casing, a 70x50 mesh was used with grid points concentrated around the axial mid−plane as well as near the solid boundaries, in order to improve resolution of the inward shear flow. Incompressible steady flow was assumed, and boundary conditions were imposed using measured values of rotational speed, inlet flow−rate and temperature. Low inlet turbulence levels were prescribed. The discrete nozzles of the experimental rigs were represented by equivalent−area annular inlets in the axisymmetric models.

Heat transfer computations were carried out using a turbulent Prandtl number of 0.9 and including the effects of viscous dissipation in solving the total enthalpy equation. Polynomials were fitted to measured surface temperatures to provide the thermal boundary condition for the heated disc for each case considered. The inner and outer cylindrical surfaces, which were insulated in the experiments, were assumed to be adiabatic. The temperature of the unheated disc was not measured, and was estimated by accounting for heat conduction through the disc. For this, the exterior surface was assumed to behave as a free−disc; Mirzaee et al [3] used the same assumptions and gave further details. The simplified surface−to−surface radiation model described by Mirzaee et al [4] was also used here in order to make consistent comparisons between the computed Nusselt numbers and the measurements of total heat transfer. Typically, the estimated radiation effects increased Nu by around 10%, but the shape of the distributions was not affected.

For verification of these computational models, comparisons were made where available with results obtained using a well−validated research code, employing the Launder−Sharma low Reynolds−number k−ε turbulence model, as also used by Mirzaee et al [3], Mirzaee et al [4] and

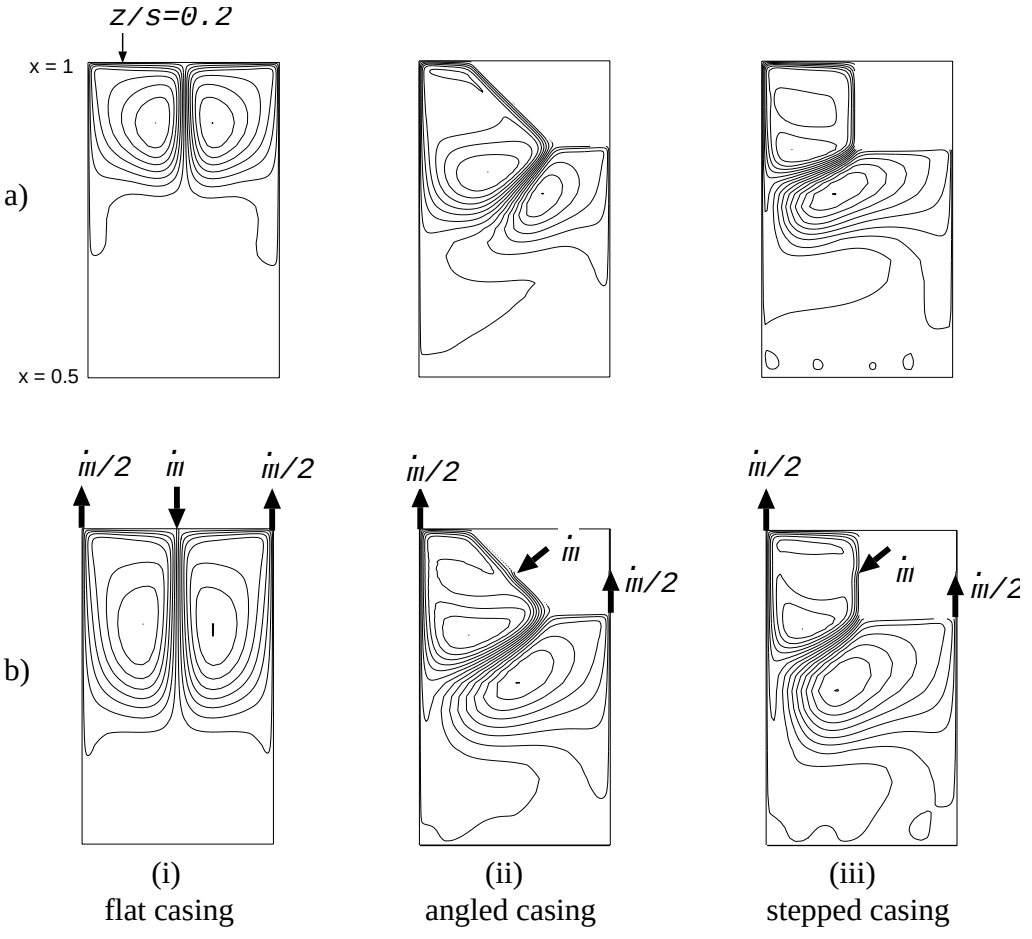

Fig. 2 Computed effect of stationary casing geometry on secondary flows for $Re_\phi = 1.5x10^6$
a) $C_w = 0$ ($\lambda_T = 0$) , b) $C_w = -3000$ ($\lambda_T = -0.034$) , c = 0

Jaafar et al [5]. Very similar computed flow structures and heat transfer levels were obtained using the two codes and models in most cases; full details are given by Jaafar [6]. (Results from the research code are not presented here, as gridding considerations prevented its application to the angled casing problems.)

COMPUTED EFFECT OF GEOMETRY ON FLOW STRUCTURE

Fig. 2 shows the computed effect of the stationary casing geometry on secondary flow streamlines, for two different values of C_w at $Re_\phi = 1.5x10^6$. For both $C_w = 0$ and $C_w = -3000$, there are clear similarities between the secondary flows for the three different configurations, despite the asymmetry introduced by the more complicated casing geometries. (The inlet arrangement in the stepped casing configuration shown in Fig. 2b(iii) is hypothetical, and considered for completeness; in experimental work using this geometry, the inlet air was introduced through holes in the heated rotating disc, as shown in Fig. 1c.)

The results for the sealed systems, $C_w = 0$ (Fig. 2a), show the fundamental effects of the outer casing on the secondary recirculations. For the flat casing, there is an inner region in near solid−body rotation for $x = r/b < 0.7$ approx. For the angled casing, the inward free shear flow is formed at the inner corner of the casing. Consequently, there is greater recirculation of flow in the inner part of the system than for the flat casing. For the stepped casing (Fig. 2a(iii)), there is rotor−stator type flow in the outer region between the left−hand disc and the radial face of the casing. Part of the inner region is occupied by the anti−clockwise recirculation set up by the free shear flow, which again forms at the inner corner of the casing.

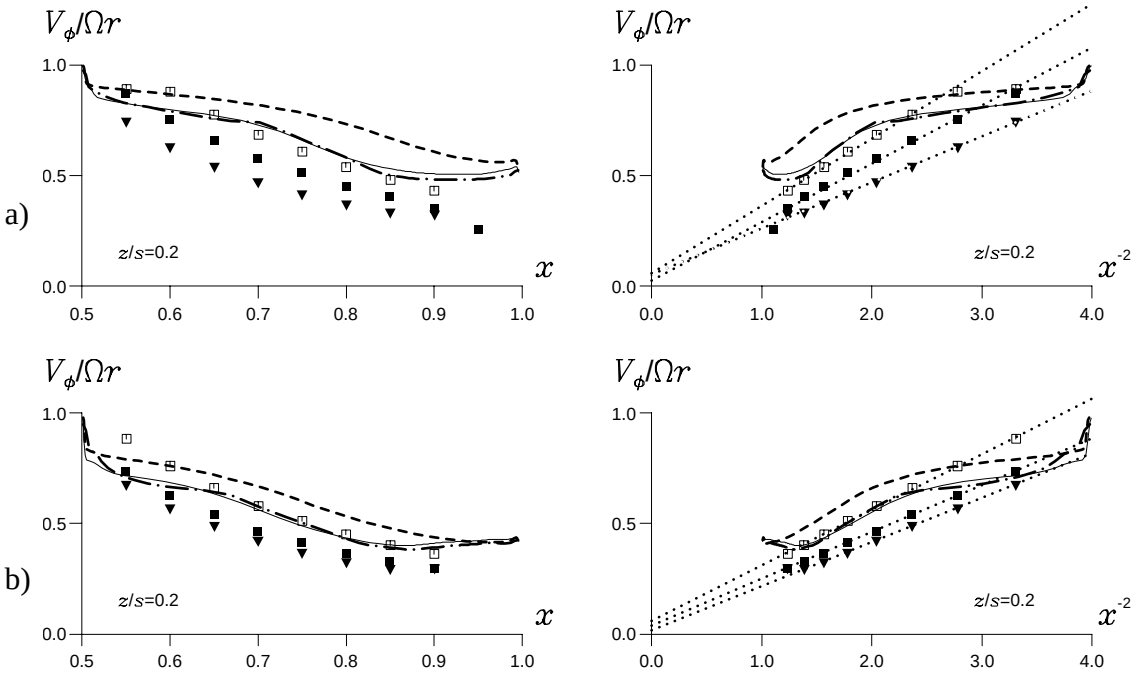

Fig. 3 Comparison between computed and measured radial distributions of tangential velocity for $Re_\phi = 1.5x10^6$; effect of stationary casing geometry
a) $C_w = 0$ ($\lambda_T = 0$), b) $C_w = -3000$ ($\lambda_T = -0.034$) (------ Rankine vortex)

casing	computed	measured
flat :	– – – –	■ "rough" surface, Gan et al [1] ❑ "smooth" surface, Mirzaee et al [3]
angled :	———	▼ "rough" surface (c = 0.07)
stepped :	—·—	

For the cases with $C_w = -3000$ (giving $\lambda_T = -0.034$) shown in Fig. 2b, the inward penetration of the secondary flows is increased, compared with the corresponding sealed case, for each of the geometries considered. The superposed flow enters with zero angular momentum (c = 0), thus reducing the levels of tangential velocity in the system and increasing the flow radially outward on the discs. The inlet flow is entrained into the boundary layer flowing radially inward along the casing for both the angled and stepped configurations. This corresponds to the "viscous regime" described by Jaafar et al [7].

Fig. 3 shows quantitative comparisons between computed radial distributions of tangential velocity and measured data for the cases illustrated in Fig. 2. The distributions are shown as $V_\phi/\Omega r$ plotted against non−dimensional radius x = r/b and against x^{-2}; for the latter, combined free and forced (or Rankine) vortex flow appears as a straight line, as explained by Gan et al [1]. The measurement location, z/s = 0.2, is outside the boundary layer on the left−hand disc; measured axial distributions showed little axial variation in V_ϕ between the boundary layers.

The computed results for the sealed systems (Fig. 3a) show that tangential velocity levels are reduced for the angled and stepped casings compared with the flat casing, due to the increased total area of the stationary surfaces for these two geometries (the computed disc moment coefficients were also found to be consistent with an increased frictional moment over the casing). The additional velocity data obtained by Mirzaee et al [3], after reducing the surface roughness of the flat casing, show that measured velocities are increased for the "smooth" surface compared with the original "rough" surface results, but that similar Rankine vortex structure is still observed. (There was no net flow through the sealed system, however it was possible that air could be ingested into the rotating cavity through the holes in the disc.)

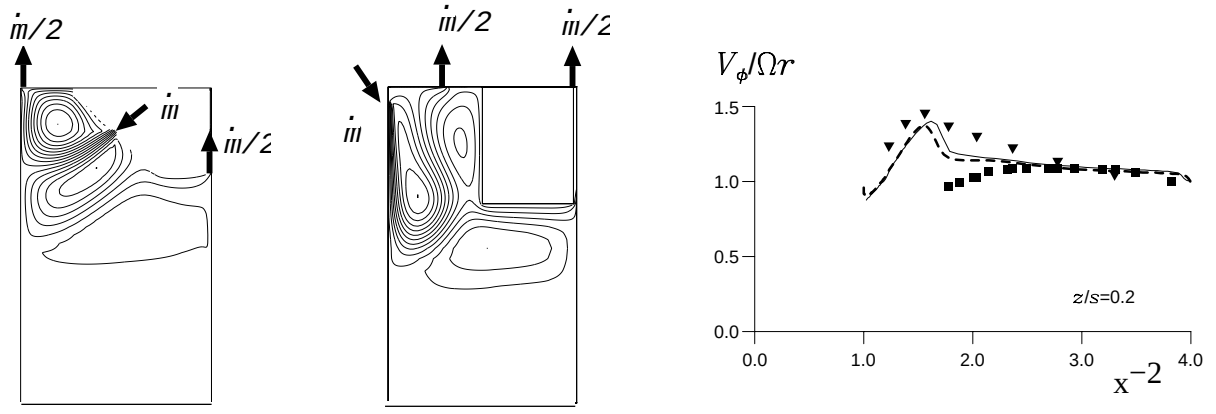

a) angled casing (c = 1.06) b) stepped casing (c = 1) c) tangential velocity distributions

Fig. 4 Effect of stationary casing geometry for $C_w = -24000$ and $c \approx 1$

		computed	measured (Jaafar et al [7])
angled casing:	$Re_\phi = 7.5 \times 10^5$ ($\lambda_T = -0.475$)	——	▼
stepped casing:	$Re_\phi = 9.4 \times 10^5$ ($\lambda_T = -0.4$)	- - - -	■

The agreement between the computed flow structure for the flat casing for $C_w = 0$ and the "smooth" surface data is poor, as also found by Mirzaee et al [3]. The use of steady, axisymmetric modelling and an isotropic turbulence model may both contribute to the discrepancies. For the angled casing, the measured results correspond to "rough" surface conditions for the casing, but poor prediction of the Rankine vortex structure is again afforded by the computations. The computed results for the stepped and angled casings coincide in the inner part of the system, and the computed effect of the casing geometry is very small even in the outer part of the system. (No velocity measurements were made for the stepped casing configuration for $C_w = 0$.)

Similar observations to those made above for cases with $C_w = 0$ apply to the results shown in Fig. 3b for $C_w = -3000$ ($|\lambda_T| = 0.034$), although there is some improvement in the comparison between computed tangential velocity levels and measured values for the "smooth" flat casing. There is again no significant difference between the computed results for the stepped and angled casings, suggesting that in the "viscous regime" (where the inlet flow is entrained into the boundary layer on the casing as shown in Fig. 2b) the flow structure is determined mainly by entrainment of fluid into the boundary layers on the rotating discs. (As mentioned above, the inlet arrangement for the stepped casing considered here is hypothetical, and no measurements are available).

Fig. 4 shows a further comparison between computed secondary flows, and computed and measured tangential velocity distributions, for two different casings for $Re_\phi = 7.5 \times 10^5$, $C_w = -24000$ ($|\lambda_T| \geq 0.4$) and $c \approx 1$. Measurements were not made for the flat casing at these conditions, and computations have not been carried out. The results shown in Fig. 4a for the angled casing correspond to the "inertial regime", identified by Jaafar et al [7], where the powerful inlet flow impinges on the left−hand disc, giving rise to outflow and inflow on the disc, radially outward and radially inward of the stagnation region respectively. The computed secondary flows shown in Fig. 4a and Fig. 4b suggest that the inward penetration of the swirling cooling air at this high flow−rate is not sensitive to the details of the casing geometry or inlet arrangements.

Fig. 4c shows the corresponding computed and measured results for the tangential velocity distributions (at z/s = 0.2). The trend of the data is reasonably well predicted for the angled casing configuration; the inner region ($x < 0.65$ or $x^{-2} > 2.5$ approx.) is in near solid−body rotation and rotating slightly faster than the discs, and in the outer region there is indication of free−vortex behaviour (rV_ϕ constant, or $V_\phi/\Omega r \propto x^{-2}$). The stepped casing computations, however, show none of the sensitivity to the changes in geometry and inlet location suggested by the measurements for

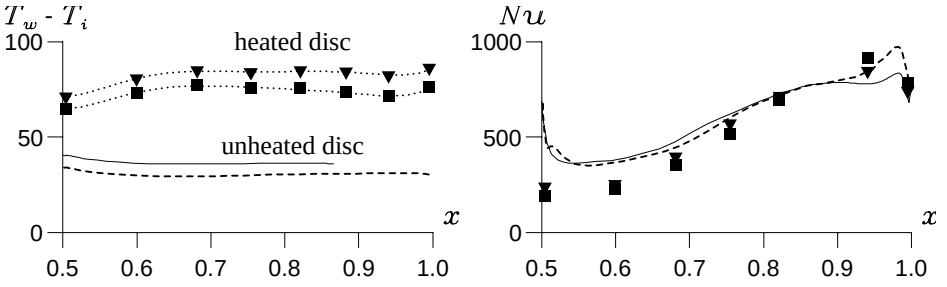

a) Comparison between flat and angled casings for $Re_\phi = 1.5x10^6$, $C_w = -3000$ ($\lambda_T = -0.034$)
computations , data: - - - - , ■ : flat casing , —— , ▼ : angled casing

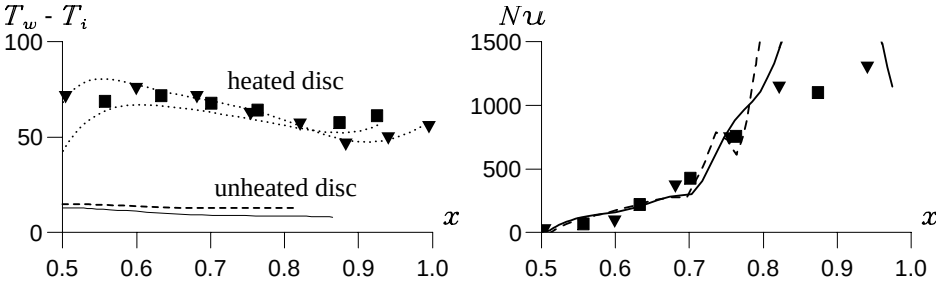

b) Comparison between stepped and angled casings for $Re_\phi = 7.5x10^5$, $C_w = -24000$ ($\lambda_T = -0.475$)
computations , data: - - - - , ■ : stepped casing , —— , ▼ : angled casing

Fig. 5 Effect of stationary casing geometry on heated disc Nu distributions

x > 0.65. Jaafar et al [7] presented other results for the angled casing configuration which suggest that the computational model used here is able to reproduce correctly the main features of the bulk flow for a range of conditions in the "inertial regime". Conversely, Jaafar et al [5] found that axisymmetric computations using k−ε turbulence models gave poor agreement with the available measured velocity distributions for the stepped casing configuration for a range of values of $|\lambda_T|$.

EFFECT OF GEOMETRY ON HEAT TRANSFER

Fig. 5 presents heat transfer results for the different casing geometries for cases related closely to those considered for the fluid dynamics comparisons. As stated above, the temperature of the unheated disc was not measured, and appropriate assumptions concerning conduction and radiation were employed for the computations. The temperatures and Nusselt numbers for the heated disc, and the computed temperatures on the unheated disc, are plotted against nondimensional radius x for each case considered. (Nusselt numbers are given by $Nu = qr/k(T_w - T_i)$, where q is the total heat flux, k the thermal conductivity of the fluid, and $T_w - T_i$ is the difference between the local heated disc surface temperature and the fluid inlet temperature, as shown in Fig. 5.)

Fig. 5a shows the comparison between Nusselt number results for the heated rotating disc for the flat and angled casings, for $Re_\phi = 1.5x10^6$, $|\lambda_T| = 0.034$ and c = 0.07. (The computed (and measured) flow structures for these cases are very similar to those shown in Fig. 2b and Fig. 3b for c = 0; the effect of the low level of inlet swirl is small.) There is little difference between either measured or computed values of Nu for the two systems; the use of fully−turbulent wall−function assumptions may contribute to the overprediction of the data for x < 0.7. Although not shown here, measured values of Nu for the stepped casing configuration at these conditions (but for which c = 1) were very similar to the data shown in Fig. 5a for the other systems, except in the vicinity of the rotating inlets (x > 0.85).

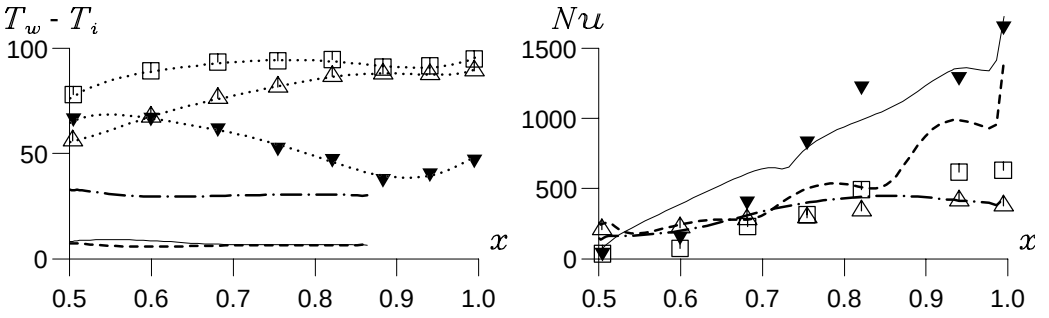

a) $Re_\phi = 3.75x10^5$

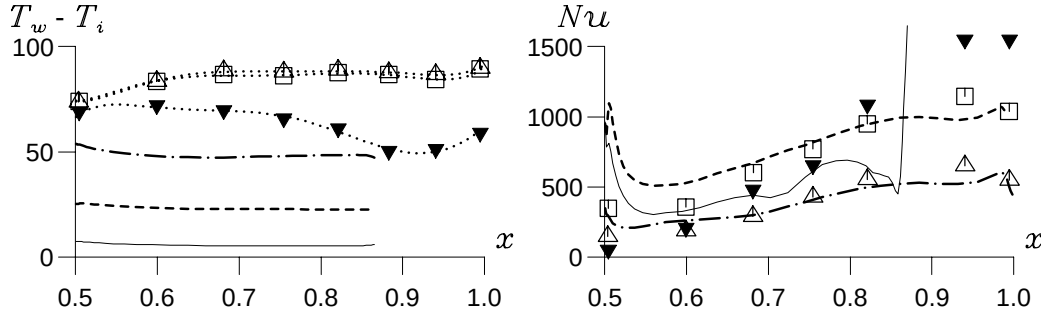

b) $Re_\phi = 1.5x10^6$

Fig. 6 Variation of heated disc Nu distributions with Re_ϕ and C_w for the angled casing geometry computations , data: —·— ,▵: C_w = −1500 , - - - - ,❑: C_w = −6000 , —— ,▼: C_w = −24000

Fig. 5b shows a comparison of results for the stepped and angled casings for a higher value of $|\lambda_T|$ (= 0.475) and c = 1, for which the flow structures are those shown in Fig. 4. Measured heat transfer rates are again very similar for the two configurations, and for these cases the computations agree well with the data in the inner part of the system. High heat transfer is computed in the outer part of both systems; in both cases, regions of stagnation and boundary layer separation occur at the disc surface which may not be computed accurately. At high values of $|\lambda_T|$ such as this, other measured Nu levels for the stepped and angled casings (not presented here) suggest that inlet swirl has a greater effect than the different casing configurations.

VARIATION OF HEAT TRANSFER FOR THE ANGLED CASING CONFIGURATION

Fig. 6 shows the variation of disc surface temperatures and heated disc Nusselt numbers with x for the angled casing geometry, for $1500 < |C_w| < 24000$, $Re_\phi = 3.75x10^5$ and $Re_\phi = 1.5x10^6$, a range which includes both the viscous and inertial regimes for this system. Jaafar et al [7] described comparisons between computed and measured radial and tangential velocity distributions for these cases.

The computations and measurements show that the peak value of Nu increases with increasing $|C_w|$ at both values of Re_ϕ, and Nu values are higher at the higher value of Re_ϕ. The agreement between the computed and measured values of Nu is reasonably good, except for the outer part of the system for C_w=−6000 in Fig. 6a and for C_w=−24000 in Fig. 6b. Both of these cases are affected by the strong recirculation and impingement effects for the inertial regime as described above. The highest value of $|\lambda_T|$ occurs for the C_w=−24000 case shown in Fig. 6a, where the measured levels of Nu are reproduced correctly for x > 0.7. The remaining cases correspond to the viscous regime, and these computations also agree well with the data.

Thus, for the viscous regime, the computations give relatively poor estimates of the tangential velocity distribution (see Fig. 3) and relatively good predictions of Nu; for the inertial regime, the converse is true (see Fig. 4). A possible explanation is that the boundary layer flow, which controls the heat transfer, is computed more accurately for the viscous regime. By contrast, the recirculating flow and impingement occurring in the inertial regime are not computed accurately by the k−ε model.

CONCLUSIONS

Comparisons have been presented between computed and measured results for a rotating cavity with a stationary outer casing in order to investigate the effect of flat, angled or stepped casing geometries and different inlet arrangements on the flow and heat transfer occurring in the system. Computations have been carried out using the commercial computational fluid dynamics code PHOENICS and a k−ε turbulence model with wall functions. In some cases, the computations repeat earlier work carried out using a different code and turbulence model.

Both the computational and experimental results suggest that the effects of geometry on flow and heat transfer are small. For cases where viscous effects are important, computed flow structures do not agree well with measured tangential velocity distributions. Heat transfer rates, however, are reasonably well predicted, suggesting that the boundary layers on the discs may be computed more accurately than the bulk recirculating flows in the cavity. This is most evident for the angled casing configuration, where tangential velocities are well predicted for "inertially−dominated" cases, while heat transfer rates are poorly reproduced in the region where flow impingement and boundary layer separation are important. Nusselt number measurements for the angled casing show that peak heat transfer rates for the heated rotating disc increase with both rotational Reynolds number, Re_ϕ , and non−dimensional flow rate, C_w; the trends are reproduced reasonably well by the computations.

ACKNOWLEDGEMENTS

The experiments described here were funded by Rolls−Royce Deutschland GmbH. The measurements were made by Dr. X. Gan, Dr. P. Quinn and Dr. F. Motallebi while at the University of Bath. Universiti Putra Malaysia provided funding for Dr Jaafar during his PhD studies.

REFERENCES

[1] Gan, X., Mirzaee, I., Owen, J. M., Rees, D. A. S. and Wilson, M. (1996) Flow in a rotating cavity with a peripheral inlet and outlet of cooling air , ASME paper 96−GT−309

[2] Owen, J. M. (2000) Flow and heat transfer in rotating−disc systems: some recent developments, Proc. 3rd Int. Symp. on Turbulence, Heat and Mass Transfer, Nagoya, pp 33−58

[3] Mirzaee, I., Gan, X., Wilson, M. and Owen, J. M. (1998) Heat transfer in a rotating cavity with a peripheral inflow and outflow of cooling air , *J. Turbomachinery*, v. 120, pp 818−823

[4] Mirzaee, I., Quinn, P., Wilson, M. and Owen, J. M. (1999) Heat transfer in a rotating cavity with a stationary stepped casing, *J. Turbomachinery*, v. 121, pp 281−287

[5] Jaafar, A. A., Motallebi, F., Wilson, M. and Owen, J. M. (2000a) Flow and heat transfer in a rotating cavity with a stationary stepped casing, ASME paper 2000−GT−281

[6] Jaafar, A. A. (2000) Flow and heat transfer in a rotating cavity with a stationary casing, PhD thesis, University of Bath, UK

[7] Jaafar, A. A., Gan, X., Wilson, M. and Owen, J. M. (2000b) Flow in a rotating cavity with a stationary angled casing, Proc. 3rd Int. Symp. on Turbulence, Heat and Mass Transfer, Nagoya, pp 653−660